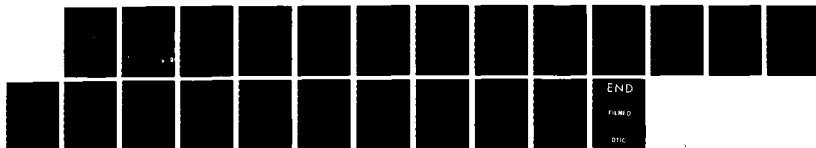


AD-A157 070 MICROWAVE FIELD STRENGTH MEASUREMENT IN A RUBIDIUM 1/1.
CLOCK CAVITY VIA ADIAB. (U) AEROSPACE CORP EL SEGUNDO
CA CHEMISTRY AND PHYSICS LAB R P FRUEHOLZ ET AL.
UNCLASSIFIED 24 JUN 85 TR-0084A(5945-05)-3 SD-TR-85-16 F/G 14/2 NL





MICROCOPY RESOLUTION TEST CHART
NATIONAL BUREAU OF STANDARDS-1963-A

AD-A157 070

**Microwave Field Strength Measurement
in a Rubidium Clock Cavity via
Adiabatic Rapid Passage**

R. P. FRUEHOLZ and J. C. CAMPARO
Chemistry and Physics Laboratory
Laboratory Operations
The Aerospace Corporation
El Segundo, CA 90245

24 June 1985

APPROVED FOR PUBLIC RELEASE;
DISTRIBUTION UNLIMITED

DTIC FILE COPY

Prepared for
SPACE DIVISION
AIR FORCE SYSTEMS COMMAND
Los Angeles Air Force Station
P.O. Box 92960, Worldway Postal Center
Los Angeles, CA 90009-2960


DTIC
ELECTE
JUL 31 1985
S A D

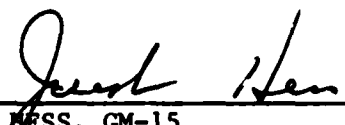
85 7 19 007

This report was submitted by The Aerospace Corporation, El Segundo, CA 90245, under Contract No. F04701-83-C-0084 with the Space Division, P.O. Box 92960, Worldway Postal Center, Los Angeles, CA 90009. It was reviewed and approved for The Aerospace Corporation by S. Feuerstein, Director, Chemistry and Physics Laboratory. Capt Matthew E. Hanson, SD/YEZ, was the project officer for the Mission-Oriented Investigation and Experimentation (MOIE) Program.

This report has been reviewed by the Public Affairs Office (PAS) and is releasable to the National Technical Information Service (NTIS). At NTIS, it will be available to the general public, including foreign nationals.

This technical report has been reviewed and is approved for publication. Publication of this report does not constitute Air Force approval of the report's findings or conclusions. It is published only for the exchange and stimulation of ideas.


MATTHEW E. HANSON, Capt, USAF
Ch, Satellite Development Branch
SD/YEZ


JOSEPH HESS, GM-15
Director, AFSTC West Coast Office
AFSTC/WCO OL-AB

UNCLASSIFIED

SECURITY CLASSIFICATION OF THIS PAGE (When Data Entered)

REPORT DOCUMENTATION PAGE		READ INSTRUCTIONS BEFORE COMPLETING FORM
1. REPORT NUMBER SD-TR-85-16	2. GOVT ACCESSION NO. A157070	3. RECIPIENT'S CATALOG NUMBER
4. TITLE (and Subtitle) MICROWAVE FIELD STRENGTH MEASUREMENT IN A RUBIDIUM CLOCK CAVITY VIA ADIABATIC RAPID PASSAGE		5. TYPE OF REPORT & PERIOD COVERED
7. AUTHOR(s) Robert P. Frueholz and James C. Camparo		6. PERFORMING ORG. REPORT NUMBER TR-0084A(5945-05)-3
9. PERFORMING ORGANIZATION NAME AND ADDRESS The Aerospace Corporation El Segundo, Calif. 90245		8. CONTRACT OR GRANT NUMBER(s) F04701-83-C-0084
11. CONTROLLING OFFICE NAME AND ADDRESS Space Division Los Angeles Air Force Station Los Angeles, Calif. 90009-2960		10. PROGRAM ELEMENT, PROJECT, TASK AREA & WORK UNIT NUMBERS
14. MONITORING AGENCY NAME & ADDRESS (if different from Controlling Office)		12. REPORT DATE 24 June 1985
		13. NUMBER OF PAGES 21
		15. SECURITY CLASS. (of this report) Unclassified
		15a. DECLASSIFICATION/DOWNGRADING SCHEDULE
16. DISTRIBUTION STATEMENT (of this Report) Approved for public release; distribution unlimited.		
17. DISTRIBUTION STATEMENT (of the abstract entered in Block 20, if different from Report)		
18. SUPPLEMENTARY NOTES		
19. KEY WORDS (Continue on reverse side if necessary and identify by block number) Adiabatic rapid passage Atomic clocks Microwave field strength		
20. ABSTRACT (Continue on reverse side if necessary and identify by block number) → Rubidium (Rb) atomic frequency standards have been found to display a strong frequency dependence on the microwave power density or field intensity. It is therefore desirable to have simple and easily applied techniques for measuring not only the field strength but also the field distribution within the clock's microwave cavity. A technique that makes use of adiabatic rapid passage (ARP) to measure field strengths in Rb clock cavities is <i>next page</i>		

DD FORM 1473
(FACSIMILE)

UNCLASSIFIED

SECURITY CLASSIFICATION OF THIS PAGE (When Data Entered)

UNCLASSIFIED

SECURITY CLASSIFICATION OF THIS PAGE(When Data Entered)

19. KEY WORDS (Continued)

20. ABSTRACT (Continued)

described and demonstrated. Measurements using this technique are found to agree with field strengths extracted by means of standard microwave procedures. The ARP technique is particularly valuable in cavities where standard microwave measurements can not be made.

UNCLASSIFIED

SECURITY CLASSIFICATION OF THIS PAGE(When Data Entered)

ACKNOWLEDGMENT

The authors wish to acknowledge the technical assistance supplied by C. M. Kahla in these studies.

[illegible]

CONTENTS

ACKNOWLEDGMENT.....	1
I. INTRODUCTION.....	5
II. FIELD STRENGTH MEASUREMENT VIA ADIABATIC RAPID PASSAGE.....	7
III. EXPERIMENTAL PROCEDURE.....	9
IV. RESULTS AND DISCUSSION.....	13
A. TE_{111} Cavity Studies.....	13
B. TE_{011} Cavity Studies.....	16
V. CONCLUSIONS.....	19
REFERENCES.....	21

FIGURES

1. Experimental Arrangement for ARP Measurements..... 10
2. Plot of ARP Signal Amplitude as a Function of Microwave
Frequency Sweep Rate for the TE_{111} Cavity..... 14
3. Plot of B_z^2 within the TE_{111} Cavity as a Function of
Radial Position..... 15

I. INTRODUCTION

The atomic frequency standard most widely used today is the passive ^{87}Rb (rubidium) gas cell frequency standard. However, studies have demonstrated that the frequency of this standard can display a strong dependence on the microwave power density or, equivalently, on microwave field intensity, within the resonance cavity.^{1,2} Consequently, it is desirable to have simple and easily applied techniques capable of measuring not only average field strengths but also the field distributions within the microwave cavity. In this report a new technique, based on adiabatic rapid passage (ARP) between the two ground-state Rb hyperfine levels, is used to measure microwave field strengths within the ^{87}Rb microwave cavity.

The measurement of microwave field strengths within the resonance cavities of Rb frequency standards is a more difficult task than might at first be anticipated. Direct measurement using various probe devices is precluded because of the glass Rb storage cell in the cavity. Furthermore, typical power reflection measurements³ can only be performed in standards in which the 6.834-GHz Rb resonance frequency is supplied directly to the cavity.⁴ The power reflection coefficient and resonance Q determined by this technique, along with a knowledge of the 6.834-GHz microwave power supplied to the cavity, can yield the microwave field distribution in the cavity.

Other commercial configurations of the Rb standard, however, do not supply 6.834 GHz directly to the cavity. Rather, these devices have step-recovery diodes as integral parts of the cavity.^{5,6} These diodes generate the required resonance frequency as a harmonic of the rf frequency supplied to them. In this common configuration the reflectance technique is then also not applicable.

Attractive alternatives to the traditional means of measuring microwave field strengths may be based on coherent techniques that directly measure the microwave Rabi frequencies of Rb atoms within the resonance cavity. The Rabi frequency, once determined, may be related directly to the strength of the microwave field.⁷ We have found Rb ARP to be a very effective means of measuring the microwave Rabi frequency.

II. FIELD STRENGTH MEASUREMENTS VIA ADIABATIC RAPID PASSAGE

ARP is a coherent transient phenomenon resulting in population reversal between two atomic or molecular levels as an electromagnetic field's frequency is swept across their resonance frequency.⁷⁻⁹ For this phenomenon to occur, the frequency sweep rate is required to be "rapid" with respect to the relaxation processes occurring in the system, and at the same time slow enough so that the system can follow the frequency sweep "adiabatically." Previously, we have investigated ARP both experimentally and theoretically in the ^{87}Rb hyperfine transition.¹⁰ For this system, optical pumping, typically supplied by a diode laser, produces a population imbalance in the ground-state hyperfine levels; the influence of a microwave frequency swept across the hyperfine resonance is monitored by the transmitted intensity of the optical pumping radiation.

As would be expected, the degree of population inversion depends on the microwave field sweep rate. The theoretical analyses of ARP in this system yielded an interesting relation between the sweep producing the maximum degree of population reversal β_m , and the microwave Rabi frequency ω_1 :

$$\omega_1^2 \approx 1.5 \beta_m \quad (1)$$

The expression was found to be accurate to better than 10% over the range of Rabi frequencies normally encountered in clock operation.

The Rb clock transition occurs between the ($F = 2, m_F = 0$) and the ($F = 1, m_F = 0$) ground-state hyperfine levels. This is a magnetic dipole transition stimulated by the z component of the magnetic portion of the electromagnetic field within the microwave cavity, B_z . Consequently, the Rabi frequency may be written as

$$\omega_1 = \frac{\mu_0 |B_z|}{h} \quad (2)$$

with μ_0 the Bohr magneton and h Planck's constant divided by 2π .

Taken together, Eqs. (1) and (2) provide a means of extracting the absolute value of the z component of the magnetic field within the cavity from ARP results. Since the mode in which the cavity oscillates is typically known, the z component of magnetic field specifies the remaining magnetic and electric field components, along with energy density. Typically, the optical pumping light probes regions of varying field strength. A question, however, arises as to how the field extracted by the ARP technique is affected by the distribution of field strength within the optically probed volume. Is an average field strength obtained, or perhaps a field strength more representative of the maximum value within the probed volume? This point is discussed subsequently.

III. EXPERIMENTAL PROCEDURE

The apparatus used to apply the ARP technique is shown in Fig. 1. A single-mode diode laser, Mitsubishi ML-4101, tuned to one of the D_1 hyperfine resonance lines at 794.7 nm, was used to pump atoms optically from the $5^2S_{1/2}$ ($F = 2$) Zeeman manifold into the $5^2S_{1/2}$ ($F = 1$) Zeeman manifold. The Doppler-broadened absorption linewidth (~ 500 MHz) was greater than both the laser linewidth (~ 100 MHz) and the Zeeman splitting (< 700 kHz). Thus optical pumping occurred from all Zeeman sublevels of the $F = 2$ hyperfine state.

The transmitted intensity of the laser through the Rb vapor was used to determine the density of atoms in the $F = 2$ level; in steady-state, in the absence of the microwave field, this intensity is a maximum. By sweeping a microwave field across the 0-0 hyperfine transition, atoms in the ($F = 1$, $m_F = 0$) state were transferred into the ($F = 2$, $m_F = 0$) state, and the resulting change in the transmitted laser intensity was a measure of the number of atoms transferred. For a fixed microwave field strength, the sweep rate of the microwave frequency was adjusted so we could observe the largest change in the transmitted light intensity. Thus, we were able to measure the sweep rate that maximized the population reversal as a function of microwave field strength or, equivalently, the microwave Rabi frequency.

In the first experiments a Corning 7070 glass absorption cell that contained an excess of natural isotopic-abundance Rb metal and 10 Torr of N_2 was situated in a TE_{111} cylindrical microwave cavity obtained from a commercial standard ($R = 1.3$ cm and $L = 3.8$ cm) and tuned to the ^{87}Rb ground-state hyperfine transition frequency, 6.834 GHz. The N_2 was present in order to quench the Rb fluorescence, and to act as a buffer to reduce the effect of collisions with the cell walls. A static magnetic field of a few hundred milligauss was applied parallel to the cavity axis in order to define the quantization axis, and to split the Zeeman levels so that only the 0-0 transition was induced by the microwave field. The cavity and cell were maintained at about 50°C . The diode laser emission was collimated by a short-focal-length lens to a diameter of ~ 1.5 cm. An aperture allowed the diameter

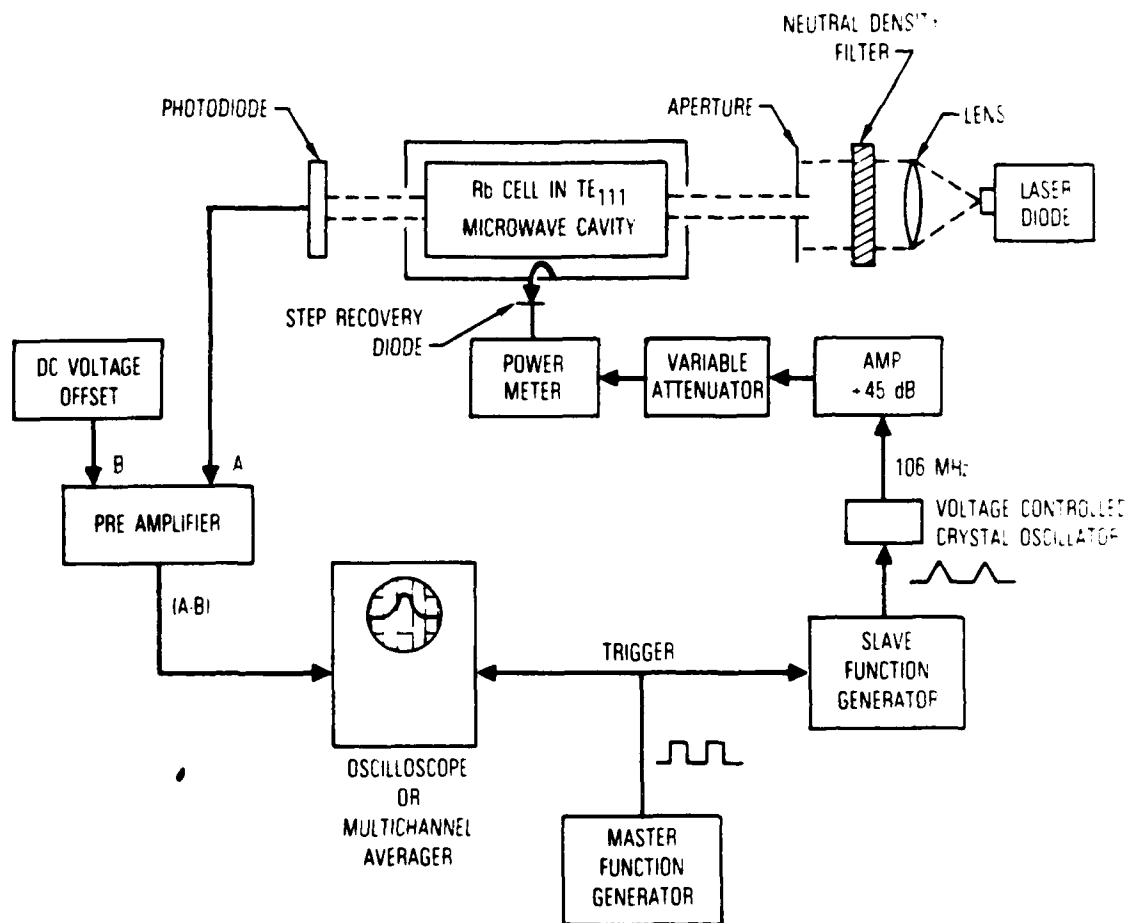


Fig. 1. Experimental Arrangement for ARP Measurements. For TE_{011} cavity studies the TE_{111} cavity, power meter, variable attenuator, and amplifier are replaced by the TE_{011} cavity, a 67 \times frequency multiplier, and a fixed attenuator.

of the laser beam entering the cavity to be varied from 0.1 cm, used for probing field strengths in specific regions, to 1.0 cm, filling the entire cavity entrance port.

The microwave frequency sweep rate was generated by applying a voltage ramp to a calibrated voltage-controlled crystal oscillator (VCXO) whose output at ~106 MHz was multiplied to the ^{87}Rb hyperfine frequency region by a step-recovery diode, an integral part of the microwave cavity. The voltage ramp amplitude and duration determined the frequency sweep rate of the 6.834-GHz microwaves, and were adjusted to produce a maximum signal amplitude on the oscilloscope. In order to guarantee that the measured β_m corresponded to a single pass through resonance, starting with the system in a steady-state condition, the ramp voltage to the VCXO was supplied by a "slave" function generator whose output was triggered every 2 sec by a "master" function generator. Since the experimentally determined pumping and relaxation times were on the order of milliseconds, steady-state conditions were attained in the time between each passage.¹⁰ For very weak signals a multichannel averager (MCA) was used to obtain the ARP signal.

Additional experiments were performed on a TE_{011} cavity ($R = 2.8$ cm and $L = 5.7$ cm) containing only ^{87}Rb . For these studies the TE_{111} cavity, step-recovery diode, power meter, and variable attenuator were replaced by an external frequency multiplier that supplied a fixed power level of 6.834-GHz radiation directly to the TE_{011} cavity. For this cavity it was possible to compare ARP field strength measurements with field strengths obtained from reflectance coefficient and cavity Q measurements.

IV. RESULTS AND DISCUSSION

A. TE₁₁₁ CAVITY STUDIES

The z component of the magnetic field in the TE₁₁₁ cavity follows the expression

$$B_z(z, r, \theta) = B J_1 \left(\frac{1.84}{R} r \right) \cos(\theta) \sin\left(\frac{\pi z}{L}\right) \quad (3)$$

Cylindrical coordinates are used, with the z axis being collinear with the cavity axis. J_1 is the Bessel function of order 1, while L and R are the length and radius, respectively, of the cavity.

As a first measurement, the laser beam was allowed to fill the entire 1-cm-diam entrance port of the cavity. In Fig. 2 the amplitude of the ARP signal as a function of microwave frequency sweep rate is displayed. β_m was found to be approximately 1.5×10^6 rad/s². Using Eqs. (1) and (2), we obtain a value of 1.7×10^{-4} G for $|B_z|$. Equation (3) indicates that the magnitude of $|B_z|$ will vary significantly over the cavity region probed by the laser beam. We wished to investigate how this ARP $|B_z|$ value was affected by the field variations within the probed region. The laser beam diameter was reduced to 0.1 cm and various radial positions were probed. The cavity was oriented in such a way that $|\cos\theta| = 1$. In Fig. 3, $|B_z|^2$, which is proportional to β_m , is shown as a function of radial position. The solid curve is the expected distribution for a TE₁₁₁ cavity. Because of the reduced beam size, these data are fairly noisy and their acquisition required the use of the MCA. The ARP data follow the expected field distribution fairly closely, except in the central region, where the measured field is larger than expected. These results show that the Rb atoms are effectively confined to relatively small regions of space because of the presence of the nitrogen buffer,^{11,12} and as far as we know represent the first direct observation of this effect in a gas cell clock's cavity. However, this localization is not perfect, as the fact that axial field strength appears not to fall to zero is believed to be due to a small motional field averaging on the part of the atoms.

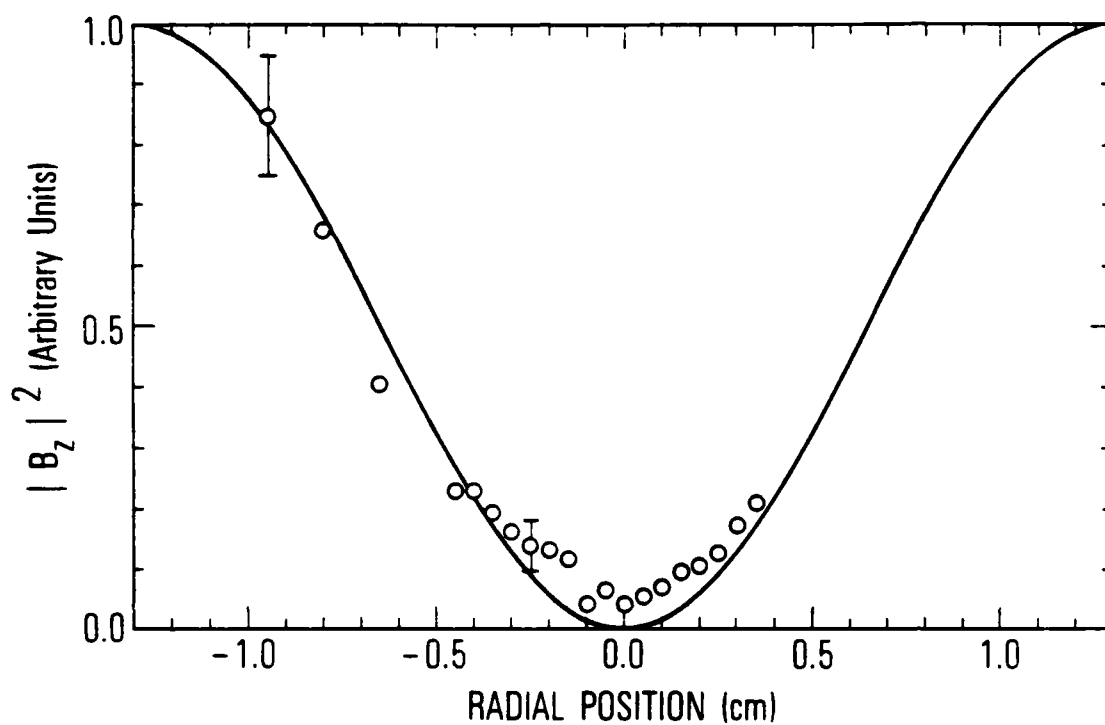


Fig. 2. Plot of ARP Signal Amplitude as a Function of Microwave Frequency Sweep Rate for the TE_{111} Cavity. The laser beam diameter was set to 1.0 cm.

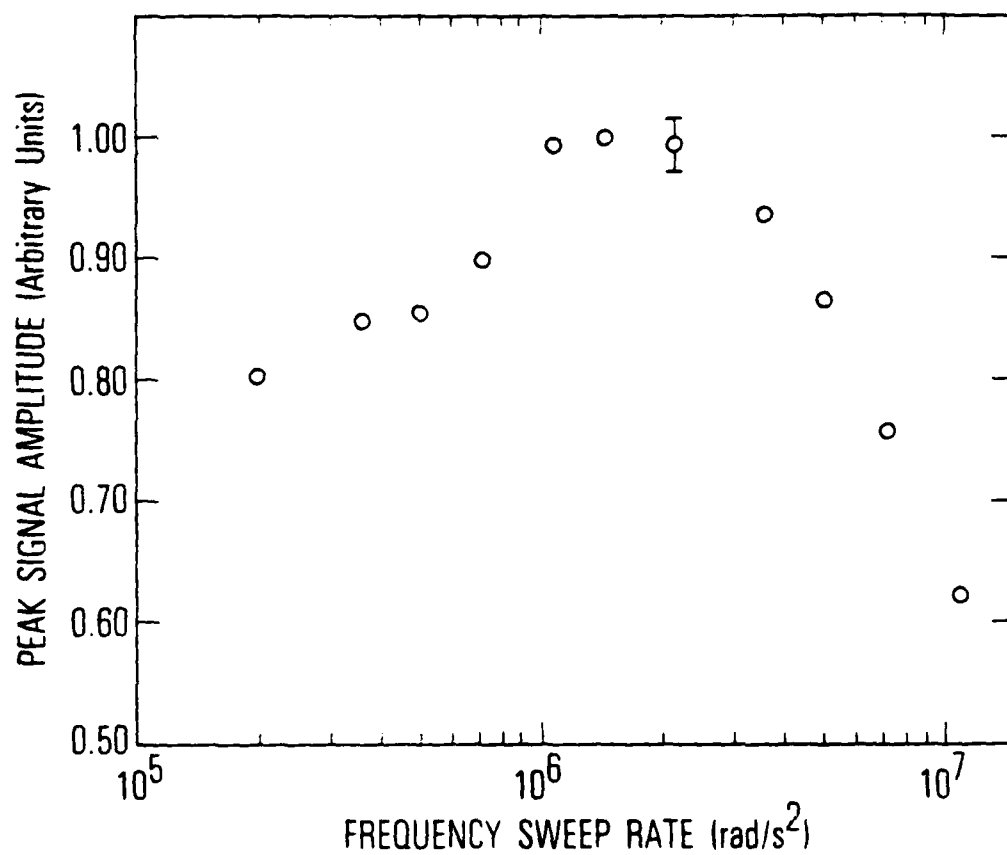


Fig. 3. Plot of B_z^2 within the TE_{111} Cavity as a Function of Radial Position.^z The laser beam diameter was 0.1 cm.

It appears that whereas a small amount of motional field averaging by the atoms is present, it is not significant, as the mode structure is clearly defined. Consequently, any field averaging observed is due primarily to the manner in which the ARP technique samples regions of different field strength. A simple average of the radial data in Fig. 3, neglecting any θ dependence, yields a field strength approximately equal to that given by the large-diameter-beam ARP measurement. We know, though, that the ARP measurement was made in a region where $|\cos\theta| = 1$. If indeed the ARP technique made a simple average, the θ dependence would require the full-beam ARP value to be less than the θ -neglected average $|B_z|$ value by a factor of about $2/\pi$. Since this is not the case, the ARP is found to weight areas of high-field more heavily than areas of low-field strength. Specifically, in this case the high-field region, where $|\cos\theta| \sim 1$, has been weighted more heavily than regions where $|\cos\theta| < 1$. A reasonable relation between the ARP field strength value and the actual fields within the volume probed by the laser beam is made, for simplicity, by taking the ARP result as falling between the average and peak field values, the intermediate value. For the cases considered here this introduces an uncertainty in absolute accuracy of the ARP technique of approximately $\pm 20\%$. This is not a problem in terms of measurement precision, because the averaging for a given cavity-cell configuration (no matter how it actually occurs) is identical from measurement to measurement.

B. TE₀₁₁ CAVITY STUDIES

As previously discussed, the TE₁₁₁ cavity did not allow comparison of the ARP field strength measurement with results from an independent measurement technique. To perform such a comparison, ARP measurements were also carried out on a TE₀₁₁-mode cavity to which 6.834-GHz radiation was directly supplied. This configuration then allowed power reflectance to be measured and cavity Q to be determined.

The z component of the magnetic field in the TE₀₁₁ cavity is given by

$$B_z(z, r, \theta) = B_{J_0} \left(\frac{3.83}{R} r \right) \sin\left(\frac{\pi z}{L}\right) \quad (4)$$

with J_0 the Bessel function of order 0. The TE_{011} cavity is attractive to study because the radial field variation near the axis is small, the principal field variation being along the cavity axis. With an entrance port diameter of 1.14 cm and a cell diameter of 5.63 cm, the field decreases only 14% from the cavity axis to the edge of the entrance port. The ARP technique was applied to the cavity, fully illuminating the entrance port with the diode laser. Making use of the ARP averaging approximation discussed previously, we could relate the raw ARP field strength to the peak value of field within the cavity, using

$$B_z^{\text{peak}} (\text{ARP}) = 3.3 \pm 1.1 \times 10^{-3} \text{ G} \quad (5)$$

The major source of the uncertainty is due to the averaging approximation. For relative measurements on similar microwave cavities, a 5 to 10% precision is attainable.

To insure that the Rb vapor in this cell was optically thin, the temperature was held at 28°C. The reduction in temperature from the 50°C of the previous measurements was necessary because of the increased length of the cell and its pure ^{87}Rb content. With an optically thin vapor the laser intensity is constant throughout the cell, providing uniform optical pumping in the probed volume. At elevated temperatures, when the vapor is no longer optically thin, optical pumping occurs more strongly at the front surface of the cell. This could lead to a preferential weighting of the field in this region. Consequently, to obtain as accurate an absolute field strength value as possible, the measurements were made at this low temperature. For relative field measurements among cavities at the same temperature, this effect would not be of concern.

Microwave power reflection measurements were also performed on the cavity containing the Rb storage cell.³ The cavity Q was found to be approximately 400, and a change in reflected power on and off microwave resonance of 1 db was observed. The power reaching the cavity during the ARP measurement was 8 mW; taken with the Q and reflected power, this value allows the calculation of the stored energy in the cavity.¹³ Additionally, the energy stored in a TE_{011} cavity may be directly related to the peak value of $|B_z|$ ¹⁴, yielding

$$B_z^{\text{peak}} \text{ (reflectance technique)} = 2.4 \pm 1.3 \times 10^{-3} \text{ G} \quad (6)$$

Within the uncertainties the two measurements are seen to agree, supporting the utility of the ARP technique and our field averaging approximation. In the application of the reflectance technique, the effect of the glass Rb storage cell on the microwave field distribution has been neglected. Whereas the storage cell effects may be calculated, an additional complication is then added to this type of measurement. The ARP technique measures the field strength directly, thus including any field perturbations induced by the storage cell.

V. CONCLUSIONS

The ARP technique has been found to be an effective means of measuring the z component of the magnetic portion of the electromagnetic field within microwave cavities typically used in Rb clocks. The technique is particularly valuable in cases where the Rb resonance frequency is not supplied directly to the cavity. In these cavities rf frequencies are multiplied to the resonance frequency by means of a step-recovery diode within the cavity, precluding the use of standard cavity field-measurement techniques. Additionally, the technique allows actual mapping of the field distribution within the cavity. Finally, we note that the capabilities of this technique are not limited exclusively to cavity applications. The technique can be applied to noncavity situations, e.g. when the microwaves are supplied through a horn.

REFERENCES

1. A. Risely and G. Busca, Proceedings of the 32nd Annual Frequency Control Symposium (1978), p. 506
2. A. Risely, S. Jarvis, Jr., and J. Vanier, J. Appl. Phys. 51, 4571 (1980).
3. G. Feher, Bell System Tech. J. 36, 449 (1957).
4. W. J. Riley, Proceedings of the 13th Annual Precise Time and Time Interval Applications and Planning Meeting (1981), p. 609.
5. H. Fruehauf, W. Weidemann, and E. Jechart, Proceedings of the 12th Annual Precise Time and Time Interval Applications and Planning Meeting (1980), p. 719.
6. H. E. Williams, T. M. Kwon, and T. McClelland, Proceedings of the 37th Annual Frequency Control Symposium (1983), p. 12.
7. A. Abragam, The Principles of Nuclear Magnetism (Oxford University Press, Oxford, 1961).
8. G. E. Pake, Paramagnetic Resonance (W. A. Benjamin, Inc., New York, 1962).
9. F. Bloch, Phys. Rev. 70, 460 (1946).
10. J. C. Camparo and R. P. Frueholz, submitted for publication to Phys. Rev. A.
11. B. S Mathur, H. Tang, and W. Happer, Phys. Rev. 17, 171 (1968).
12. J. C. Camparo, R. P. Frueholz, and C. H. Volk, Phys. Rev. A 27, 1914 (1983).
13. J. D. Jackson, Classical Electrodynamics (J. Wiley and Sons, Inc., New York, 1962), p. 256.
14. R. A. Waldron, Theory of Guided Electromagnetic Waves (Van Nostrand Reinhold Co., London, 1969), p. 278.

LABORATORY OPERATIONS

The Laboratory Operations of The Aerospace Corporation is conducting experimental and theoretical investigations necessary for the evaluation and application of scientific advances to new military space systems. Versatility and flexibility have been developed to a high degree by the laboratory personnel in dealing with the many problems encountered in the nation's rapidly developing space systems. Expertise in the latest scientific developments is vital to the accomplishment of tasks related to these problems. The laboratories that contribute to this research are:

Aerophysics Laboratory: Launch vehicle and reentry fluid mechanics, heat transfer and flight dynamics; chemical and electric propulsion, propellant chemistry, environmental hazards, trace detection; spacecraft structural mechanics, contamination, thermal and structural control; high temperature thermomechanics, gas kinetics and radiation; cw and pulsed laser development including chemical kinetics, spectroscopy, optical resonators, beam control, atmospheric propagation, laser effects and countermeasures.

Chemistry and Physics Laboratory: Atmospheric chemical reactions, atmospheric optics, light scattering, state-specific chemical reactions and radiation transport in rocket plumes, applied laser spectroscopy, laser chemistry, laser optoelectronics, solar cell physics, battery electrochemistry, space vacuum and radiation effects on materials, lubrication and surface phenomena, thermionic emission, photosensitive materials and detectors, atomic frequency standards, and environmental chemistry.

Computer Science Laboratory: Program verification, program translation, performance-sensitive system design, distributed architectures for spaceborne computers, fault-tolerant computer systems, artificial intelligence and microelectronics applications.

Electronics Research Laboratory: Microelectronics, GaAs low noise and power devices, semiconductor lasers, electromagnetic and optical propagation phenomena, quantum electronics, laser communications, lidar, and electro-optics; communication sciences, applied electronics, semiconductor crystal and device physics, radiometric imaging; millimeter wave, microwave technology, and RF systems research.

Materials Sciences Laboratory: Development of new materials: metal matrix composites, polymers, and new forms of carbon; nondestructive evaluation, component failure analysis and reliability; fracture mechanics and stress corrosion; analysis and evaluation of materials at cryogenic and elevated temperatures as well as in space and enemy-induced environments.

Space Sciences Laboratory: Magnetospheric, auroral and cosmic ray physics, wave-particle interactions, magnetospheric plasma waves; atmospheric and ionospheric physics, density and composition of the upper atmosphere, remote sensing using atmospheric radiation; solar physics, infrared astronomy, infrared signature analysis; effects of solar activity, magnetic storms and nuclear explosions on the earth's atmosphere, ionosphere and magnetosphere; effects of electromagnetic and particulate radiations on space systems; space instrumentation.

END

FILMED

9-85

DTIC